Supplementary Information

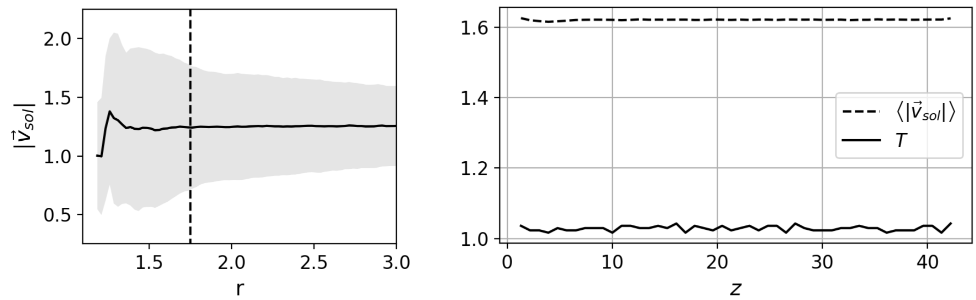

Figure 1: **Left**: Passive colloids boundary condition in bulk without gravity. **Right**: Temperature profile along the vertical and average norm of the solvent velocity in the passive colloidal dispersion under gravity $F_g = 34$.

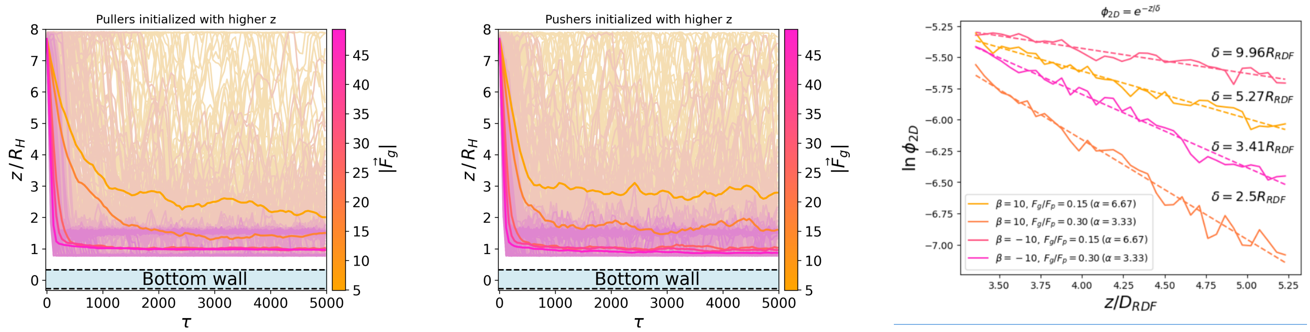

Figure 2: **Left and center**: Sedimentation trajectories (light colors) and their average (dark colors) for the 100 topmost initialized colloids. **Right**: Sedimentation lengths, δ, computed by fitting sedimentation profile in the shown range to $\phi_{2D} = e^{z/\delta}$. In the legend α is just the inverse of F_g/F_p to compare with [1].

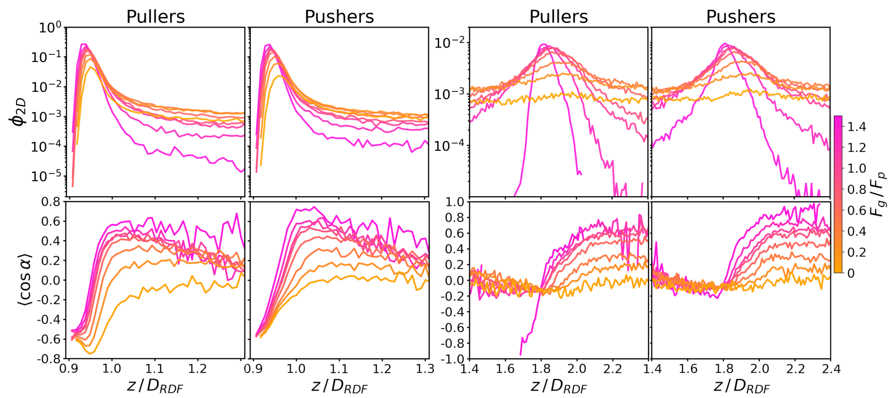

Figure 3: **Left**: Zoom on first layer using a bin width of $\Delta z = 0.044$. **Right**: Zoom on second layer using a bin width of $\Delta z = 0.044$.

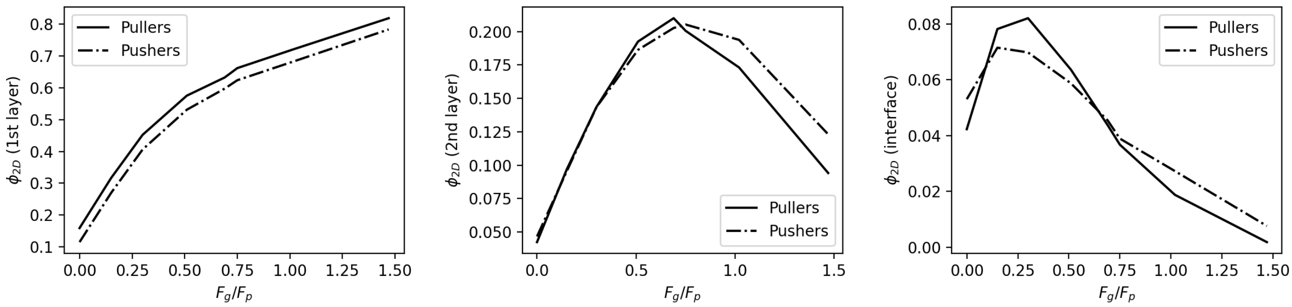

Figure 4: Maxima of the two dimensional packing fraction for 1st layer (left), the 2nd layer (center) and the interface between both (right). These plots were obtained using a bin width equal to the colloids radius estimated via RDF, $\Delta z = R_{RDF} \approx 2.1$,

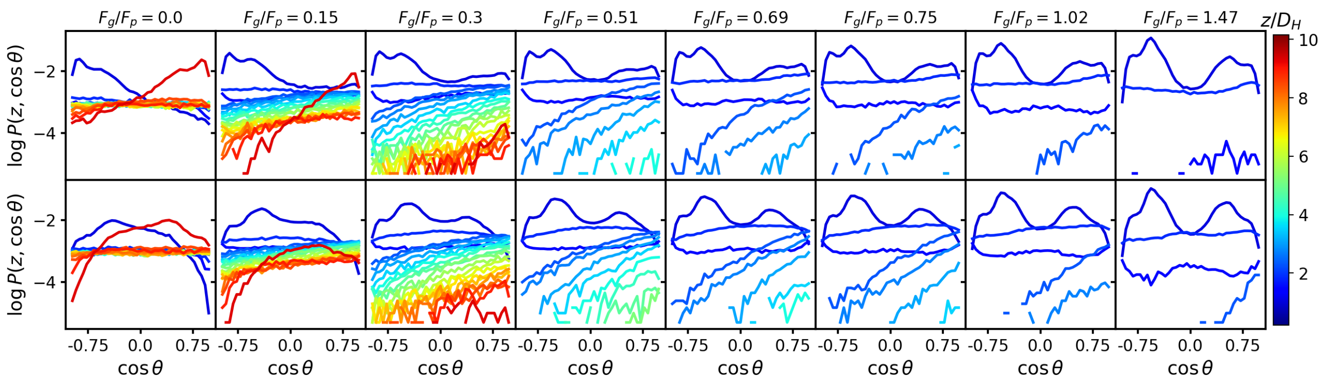

Figure 5: **Top row**: pullers. **Bottom row**: pushers. To be compared with fig. 6 of ref. [2], fig. 11 of ref. [3], fig. 2 of ref. [4] and fig. 2 of ref. [5].

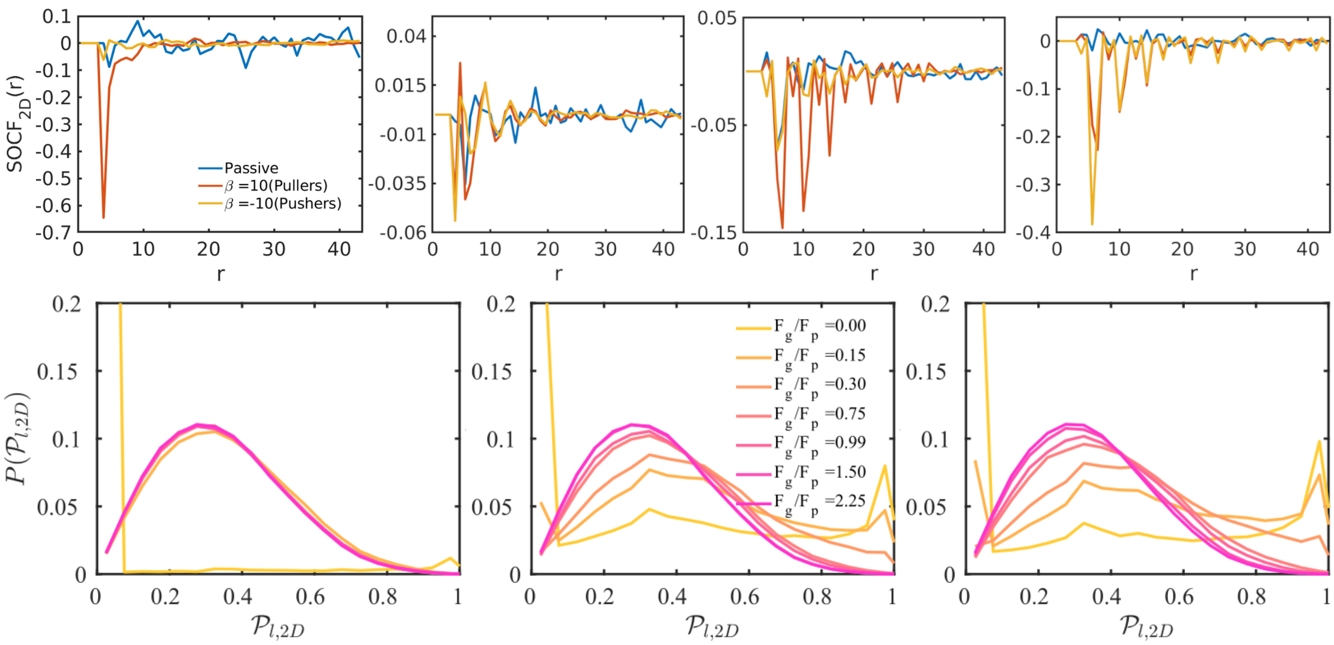

Figure 6: **Top:** The spatial orientation correlation functions computed with the projection of the orientation of the squirmers onto the xy plane. From left to right: $F_g/F_p = 0.0$, 0.75, 1.5, 2.25. **Bottom:** Distributions for local polarization computed with the projection of the orientation of the squirmers onto the xy plane for passive (left), pullers (center) and pushers (right).

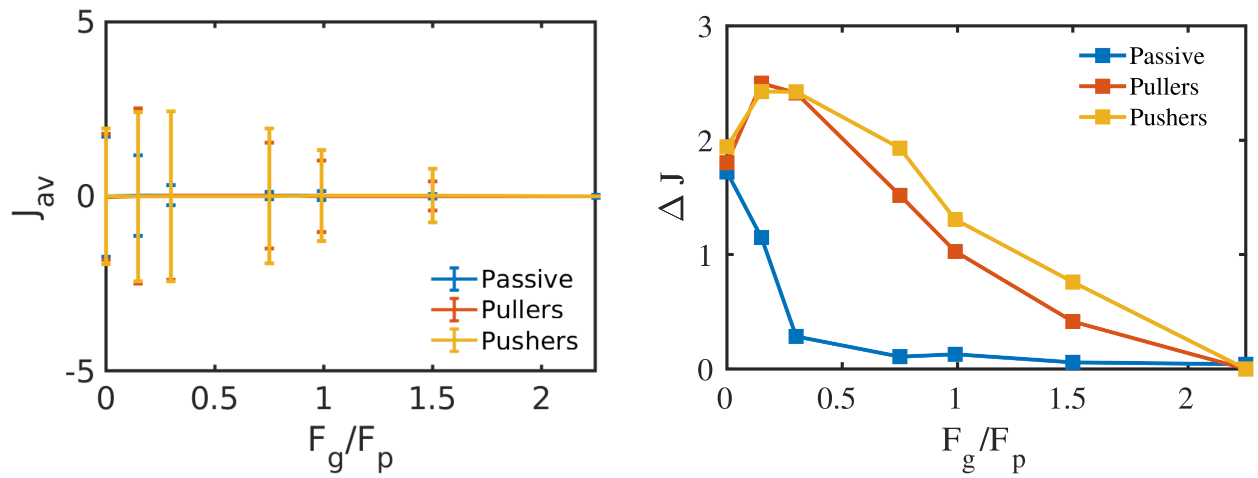

Figure 7: Average (left) and standard deviation (right) of the total flux of particles entering or leaving the bottom layer.

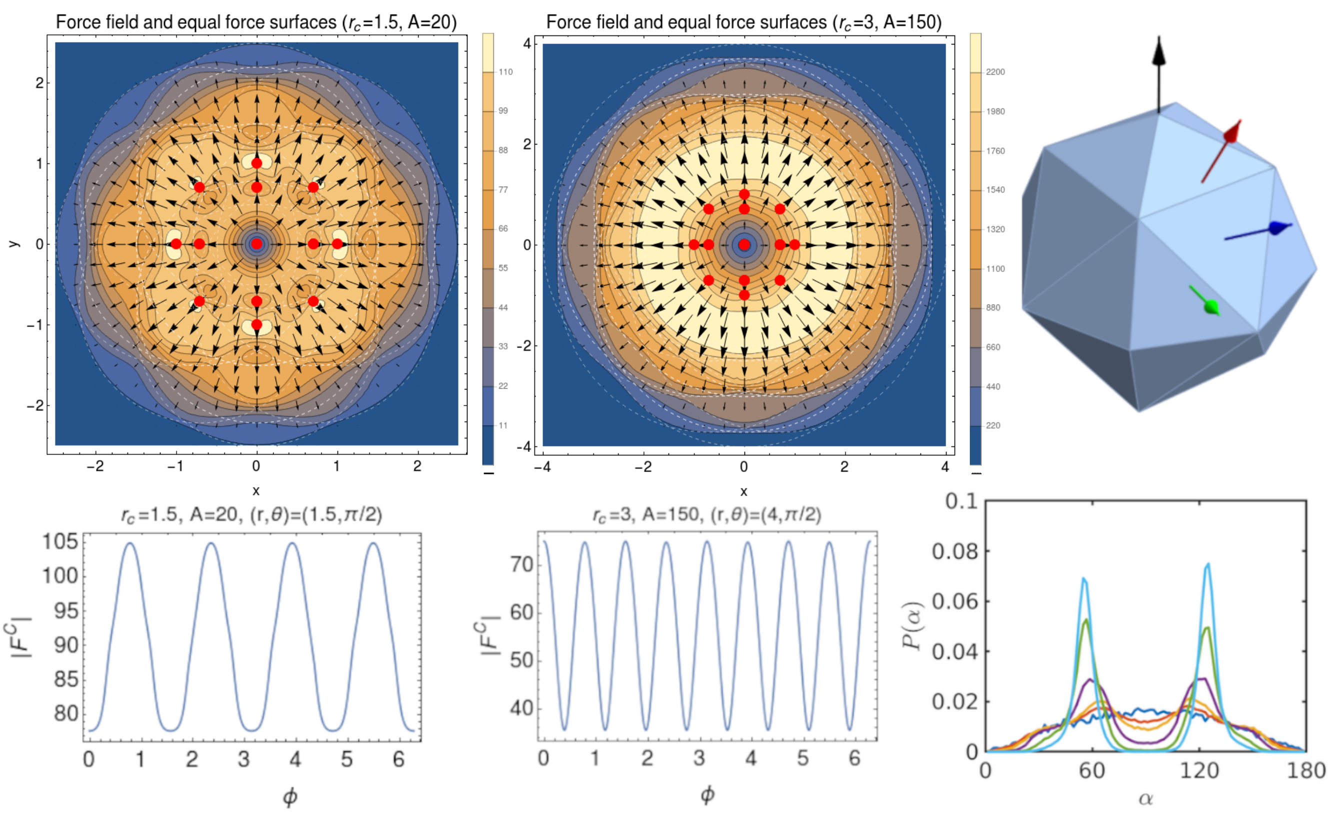

Figure 8: **Top:** Equatorial section of the force field generated by the conservative interaction of the raspberry colloid composed of 19 particles (red dots) for a DPD cutoff of $r_c = 1.5$, $A = 20$ (left) and $r_c = 3$, $A = 150$ (center). Polyhedral structure of the colloid (right), the filler particles are placed at the vertices of this polyhedron. The black arrow is the orientation of the colloid, the red, green and blue ones correspond to the normal direction of each polyhedron face, the rest of the faces are symmetric to one of these. The angles between the color arrows and the vertical (black arrow) are: 30.4º (red), 54.7º (blue) and 69.1º (green). The angles formed by the normals of the faces symmetric to the previous ones are obtained by substracting the angles to 180º: 149.6º (red), 125.3º (blue) and 110.9º (green). At first sight the most stable resting position of such a polyhedron under gravity is the face corresponding to the blue arrow. **Bottom:** Force along the equatorial coordinate ϕ at the r and θ shown in the plots label for the previous cases (left and center). Distribution of orientation angle w.r.t. the wall normal for passive colloids for increasing gravitational field (as F_g increases the two peaks start to develop).

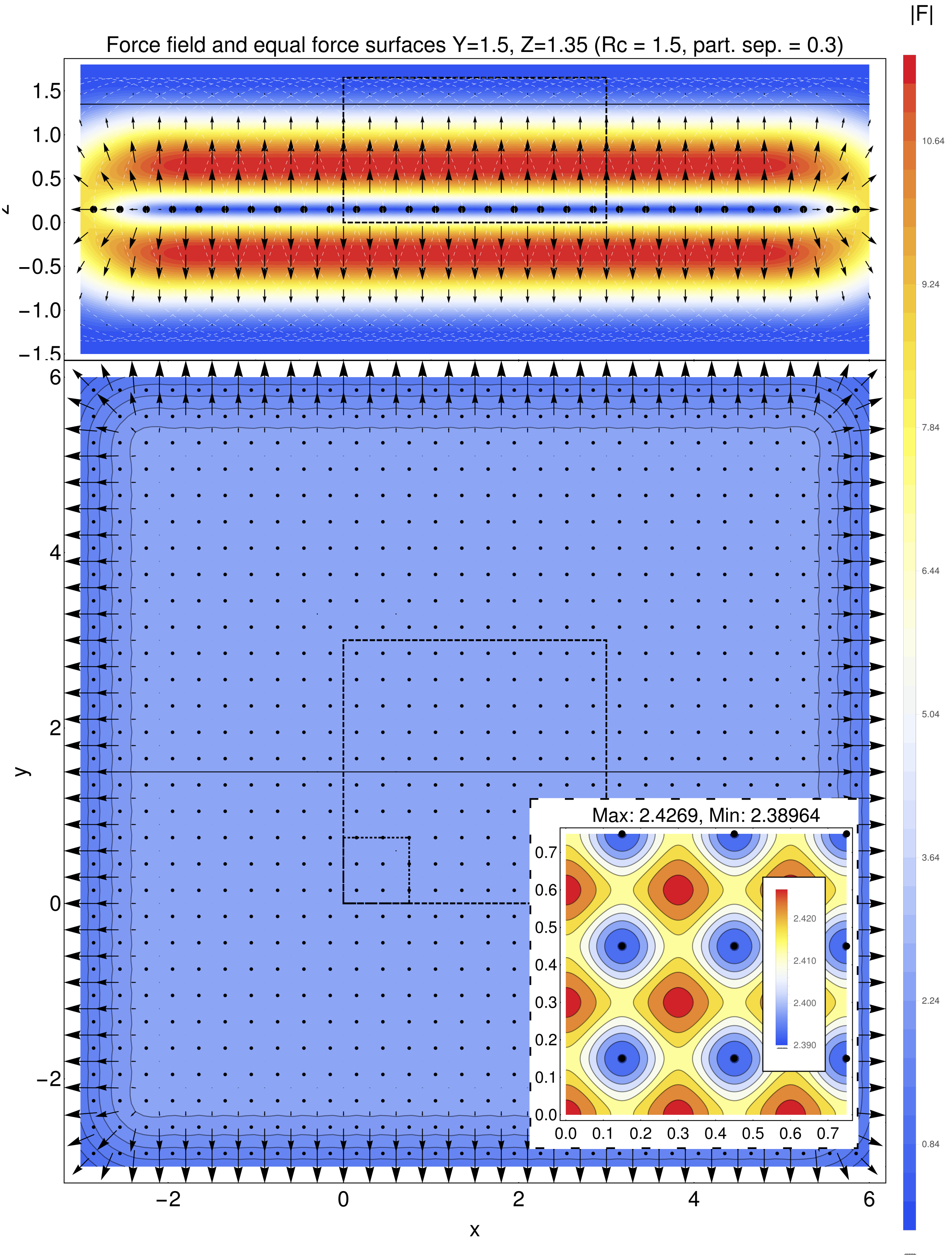

Figure 9: DPD conservative force field and equal force surfaces (color) for smaller a wall region (dashed rectangle) of 10 particles (black dots) by side with their 8 periodic images to the sides. **Top:** XZ section for $y = 1.5$. An homogenous upward repulsive force is observed. **Bottom:** XY section at $z = 1.35$. **Inset**: zoom on the lower left corner of the wall, showing wall rugosity and maximum and minimum values of the force.

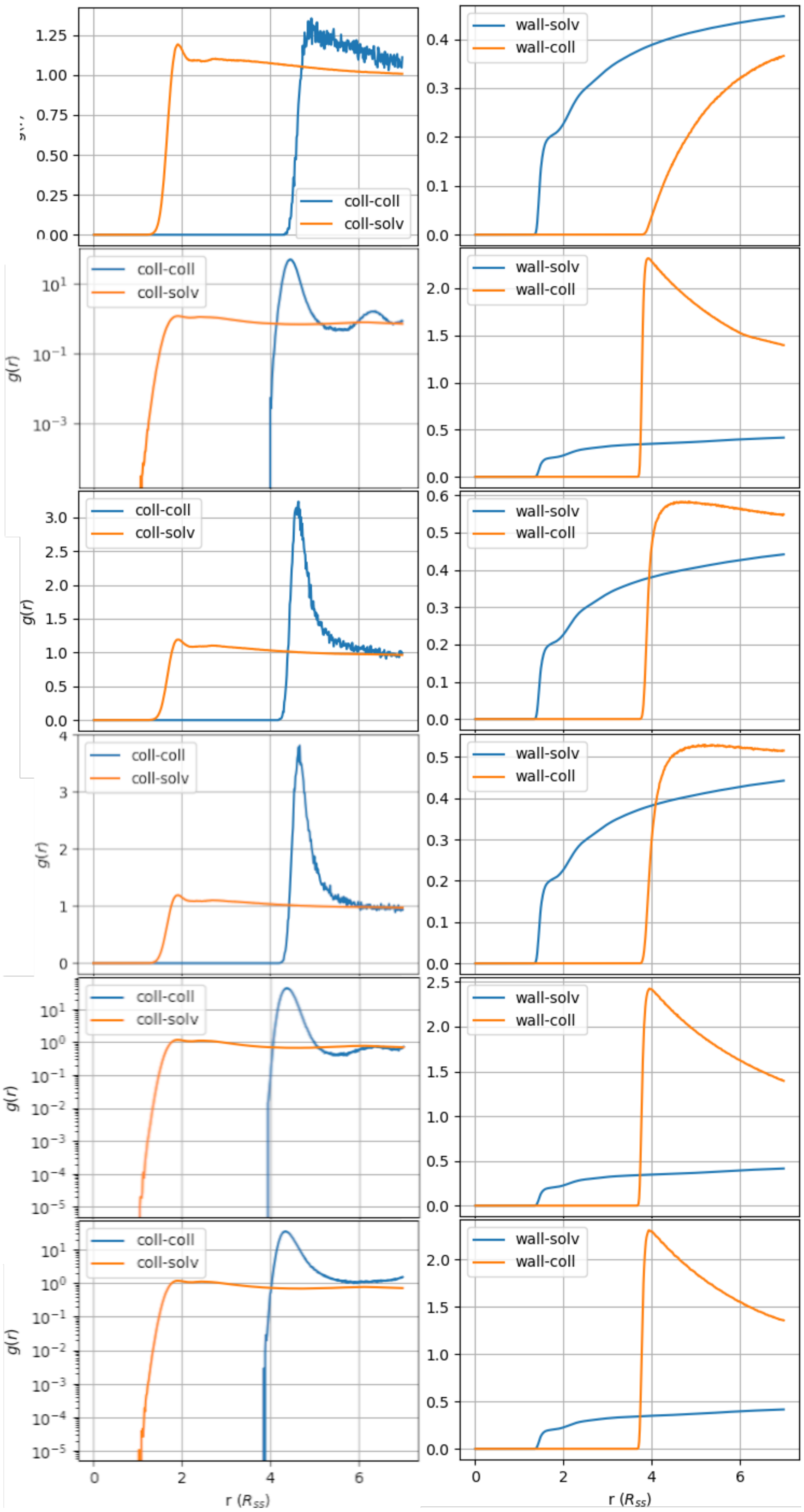

Figure 10: Radial distribution functions. **Left**: for colloids. **Right**: for walls.
1st row: passive case without gravity. **2nd row:** passive case for $F_g = 50$.
3rd row: Pullers $F_p = 16.67$ case for $F_g = 0.0$. **4th row:** Pushers $F_p = 16.67$ case for $F_g = 0.0$.
5th row: Pullers $F_p = 33.33$ case for $F_g = 50$. **6th row:** Pushers $F_p = 33.33$ case for $F_g = 50$.

References

[1] Jan-Timm Kuhr, Johannes Blaschke, Felix Rühle, and Holger Stark. Collective sedimentation of squirmers under gravity. *Soft Matter*, 13(41):7548–7555, 2017.

[2] Andrea Scagliarini and Ignacio Pagonabarraga. Hydrodynamic and geometric effects in the sedimentation of model run-and-tumble microswimmers. *Soft Matter*, 18(12):2407–2413, 2022.

[3] Gao-Jin Li and Arezoo M. Ardekani. Hydrodynamic interaction of microswimmers near a wall. *Physical Review E*, 90(1):013010, July 2014. ISSN 1539-3755, 1550-2376. doi: 10.1103/PhysRevE.90.013010. URL https://link.aps.org/doi/10.1103/PhysRevE.90.013010.

[4] Jan-Timm Kuhr, Felix Rühle, and Holger Stark. Collective dynamics in a monolayer of squirmers confined to a boundary by gravity. *Soft Matter*, 15(28):5685–5694, 2019.

[5] Mihaela Enculescu and Holger Stark. Active Colloidal Suspensions Exhibit Polar Order under Gravity. *Physical Review Letters*, 107(5):058301, July 2011. ISSN 0031-9007, 1079-7114. doi: 10.1103/PhysRevLett.107.058301. URL https://link.aps.org/doi/10.1103/PhysRevLett.107.058301.